Group velocity of electrons in 4H-SiC from Density Functional Theory simulations

Group velocity of electrons in 4H-SiC from Density Functional Theory simulations

Luigi Balestra[a,b,*], Susanna Reggiani[a,b], Elena Gnani[a,b], Antonio Gnudi[a,b]

[a] *Advanced Research Center on Electronic Systems "E. De Castro" (ARCES), University of Bologna, 40136, Bologna, Italy*
[b] *Department of Electrical, Electronic and Information Engineering (DEI), University of Bologna, 40136, Bologna, Italy*

Abstract

Silicon carbide (SiC) power MOSFETs actually represent the heart of power electronic converters due to the superior properties of SiC. However, they are affected by reliability issues which can lead to a reduction of the converter ruggedness. For this reason, it is fundamental to predict the long-term stability of the device performance in terms of threshold voltage and on-resistance drifts. In this perspective, TCAD simulations can be a very useful tool for the understanding of the phenomena that dominate such degradation mechanisms. The models actually available in the TCAD deck for the degradation analysis require the knowledge of the density of states and group velocity of the semiconductor under investigation as they are based on the direct solution of the Boltzmann equation. Despite several works are available in literature on the electronic properties of 4H-SiC, the group velocity has never been reported. In this work, it has been calculated by using the Density Functional Theory (DFT).

Keywords: Density Functional Theory (DFT), Group Velocity, 4H-SiC, Hot-Carrier Stress, Power MOSFETs

1. Introduction

Silicon-carbide (SiC) power MOSFET are nowadays considered a valid alternative to their silicon counterpart due to the attractive material properties of SiC. As a wide band-gap semiconductor, it is characterized by high breakdown field and thermal conductivity when compared with Si. This results in superior voltage rating and increased high-temperature operation capability [1]. Ruggedness and long-term reliability are fundamental for such devices in order to be successfully integrated into industrial applications such as electric vehicles and renewable energy conversion. In [2], a significant degradation of the device performance in terms of threshold-voltage shift and on-state current has been reported as a consequence of repetitive short circuit tests. It has been assumed that a significant formation of traps at the SiC/SiO_2 interface and in the oxide bulk might be caused by hot-carriers injected from the SiC bulk toward the gate oxide. Recently, a model that accurately describes the physical mechanisms that dominate such hot-carrier phenomena for Silicon has been incorporated in the framework of the Synopsys TCAD tools [3]. It accounts for both single-electrons (SE) and multiple-electron (ME) processes. Both are characterized by a reaction rate which can be expressed as:

$$k_{SE/ME}(E_{SE/ME}) = \int_{E_{SE/ME}}^{\infty} f(E)g(e)u_g(E)\sigma_{SE/ME}(E)dE \tag{1}$$

where $f(E)$ is the electron density distribution function, $g(E)$ and $u_g(E)$ are density of states and group velocity and $\sigma_{SE/ME}(E)$ is the SE/ME reaction cross-section as defined in [3]. In order to perform such kind of degradation simulations, $f(E)$ must be determined from the solution of the Boltzmann transport equation (BTE). To this purpose, the BTE solver implemented in the TCAD tool can be used, which is based on the spherical harmonics expansion [4]:

$$-\boldsymbol{\nabla}\cdot\left[\frac{u_g^2(\boldsymbol{r},E)}{3}\tau(\boldsymbol{r},E)g(\boldsymbol{r},E)\boldsymbol{\nabla}f(\boldsymbol{r},E)\right] = g(\boldsymbol{r},E)s(\boldsymbol{r},E) \tag{2}$$

where $1/\tau$ is the total scattering rate and s is the net in-scattering rate due to inelastic scattering and generation-recombination processes. The former accounts for the description of the most relevant scattering mechanisms as usually addressed in Monte-Carlo simulations [5][6], the latter can be expressed as a function of f and τ. While $g(E)$ has been already reported in different works based on DFT calculations, $u_g(E)$ is still not available to the scientific community. In this work, we calculated $u_g(E)$ for electrons in 4H-SiC starting from DFT simulations.

*Corresponding author
Email address: luigi.balestra5@unibo.it (Luigi Balestra)

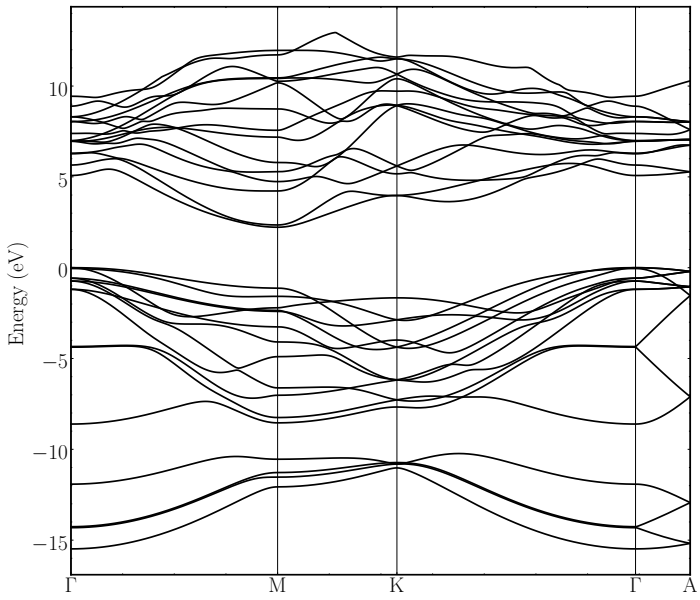

Figure 1: Band structure of 4H-SiC calculated with Quantum Espresso.

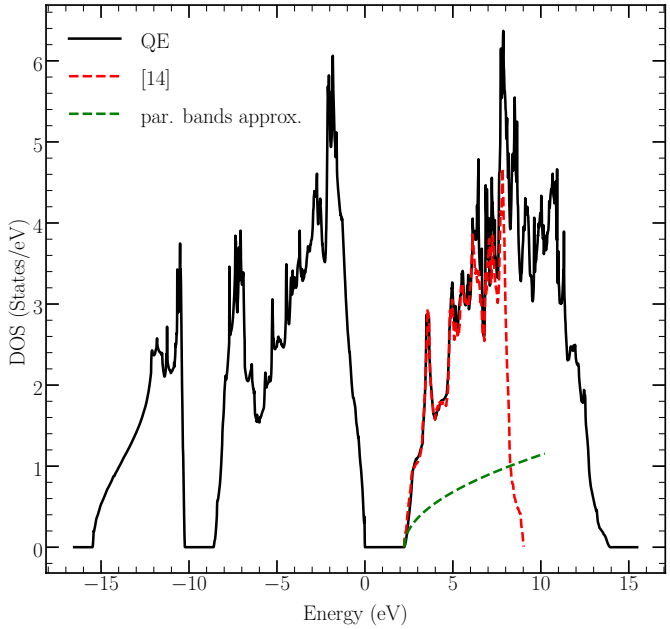

Figure 2: Density of states of 4H-SiC. Solid line: Quantum Espresso. Dashed line: calculated according to [14]. Green dashed line: parabolic band approximation. The zero is taken at the valence band maximum.

2. Group Velocity Calculation

The electronic properties of 4H-SiC have been calculated using density functional theory (DFT). The QUANTUM ESPRESSO package [7] has been used for the band structure calculations using the general gradient approximation (GGA) as parametrized by Perdew, Burke and Ernzerhof (PBE) [8]. The full band structure of 4H-SiC is reported in Fig. 1 and exhibits an energy-gap E_g of approximately 2.2eV, which is significantly lower when compared with experimental measurements. Nevertheless, it is in nice agreement with previous works in literature concerning GGA-DFT simulations of 4H-SiC[9][10]. The underestimation of E_g, a very well know problem of DFT calculations, can be solved employing hybrid pseudo-potential as shown in [11].

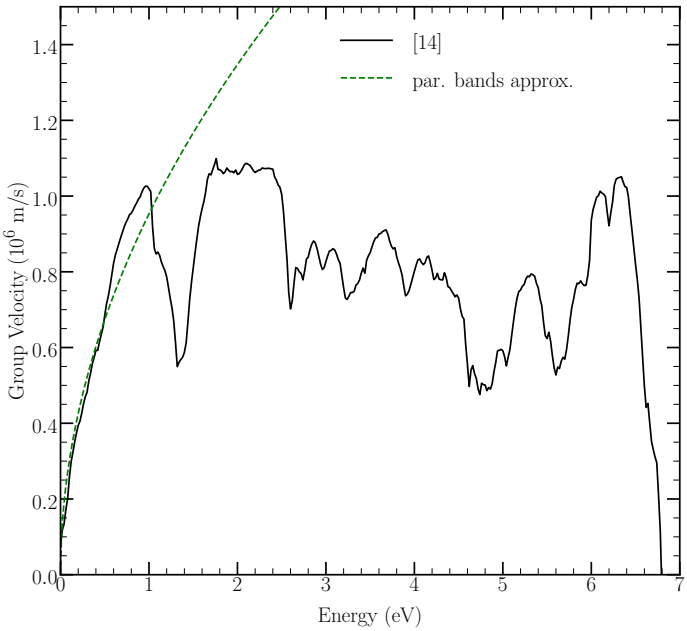

Figure 3: Group velocity of 4H-SiC. Black solid line: calculated according to [14]. Green dashed line: parabolic band approximation. The zero is taken at the conduction band minimum.

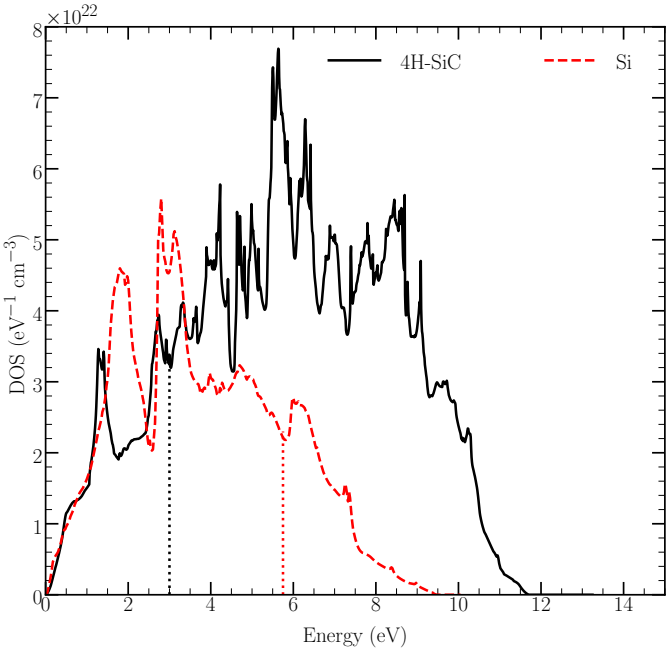

Figure 4: Electron density of states of 4H-SiC and Silicon calculated with Quantum Espresso. Vertical dotted lines represent the maximum value of energy at which the approximation with $N_B = 4$ is valid. The zero is taken at the conduction band minimum.

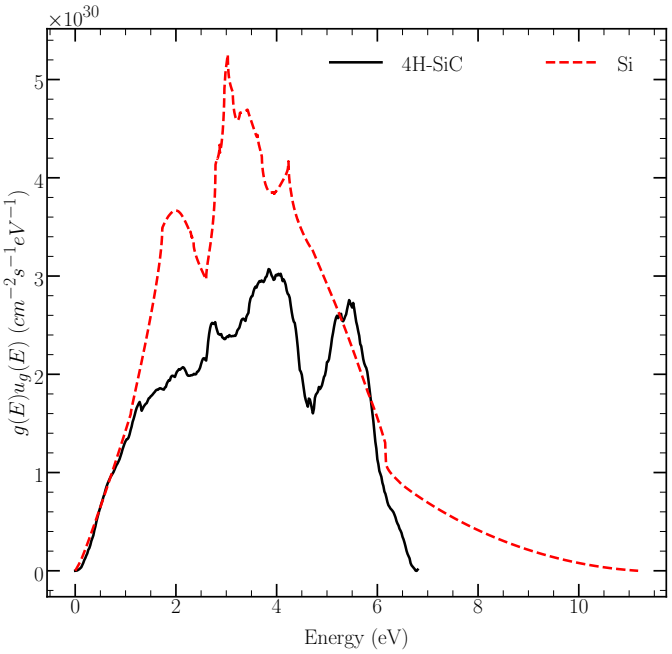

Figure 5: Product $g(E)u_g(E)$ of 4H-SiC and Silicon. The zero is taken at the conduction band minimum.

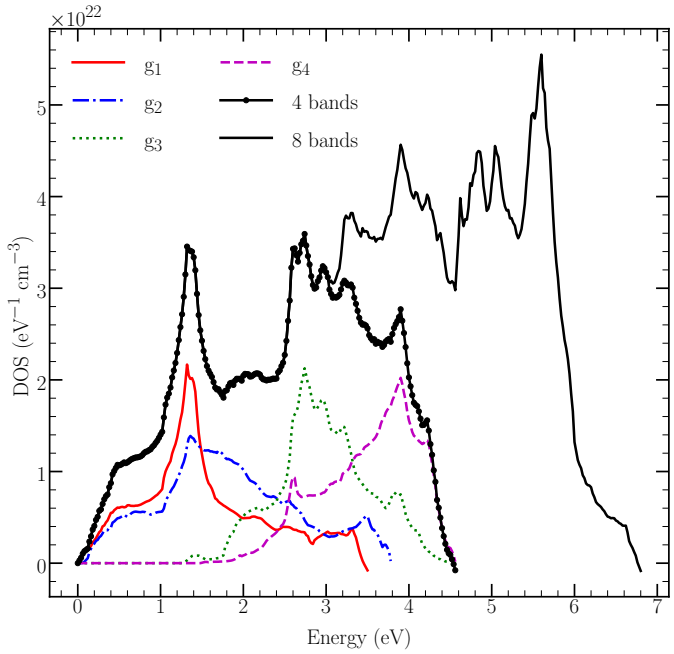

Figure 6: Density of states of 4H-SiC calculated according to [14]. Lines corresponding to g_1, g_2, g_3 and g_4 show the contribution of the first 4 bands to $g(E)$, respectively. Black line with circles: density of states obtained by summing the contribution of the first 4 bands. Black solid line: $g(E)$ calculated accounting for 8 conduction bands.

Effective masses				
	$m_{M\Gamma}$	m_{MK}	m_{ML}	$m_\perp$
This Work	0.59	0.30	0.33	0.42
[12]	n.a.	n.a.	0.29	0.42
[13]	n.a.	n.a.	0.33	0.42

Table 1: Effective masses extracted from DFT calculations ($m_\perp = \sqrt{m_{M\Gamma} m_{MK}}$).

However, this leads to a strong increase of the computational cost without significant change in the structure of the conduction bands. This is confirmed by the comparison of the calculated effective masses with the corresponding values reported in literature [12][13] as shown in Table 1. Moreover, the accurate estimation of the energy gap is not relevant for the present analysis since the calculation of u_g is not affected by a constant shift of the energetic levels. The required integration over the angles for the term $u_g^2(E)g(E)$ in Eq. 2 has been carried out following [14]:

$$u_g^2(E)g(E) = \frac{2}{(2\pi)^3} \sum_i \int_k u_i^2(\boldsymbol{k}) \delta(E - E_i(\boldsymbol{k})) d\boldsymbol{k} \qquad (3)$$

where $1/(2\pi)^3$ is the density of states in the $(\boldsymbol{r}, \boldsymbol{k})$ space, i is the band index, $u_i = (1/\hbar)\boldsymbol{\nabla} E_i$. The factor 2 accounts for the spin degeneracy. The Wannier90 tool [15] has then been used to sample the first octant of the Brillouin zone and extract the corresponding values of the energies and their first derivatives without solving the Kohn-Sham equations in a large number of k-points. In order to check the validity of the approach, the band structures calculated with Wannier90 has been compared with that obtained using Quantum Espresso. A perfect agreement between full DFT and interpolated bands has been found. In this way, higher accuracy can be obtained when compared to the second-order finite difference method shown in [14]. However, second derivatives are still obtained from standard numerical calculations. In Fig. 2, the $g(E)$ calculated with Quantum Espresso is compared with the one calculated according to [14] taking into account only 8 conduction bands. In the range 0-7eV, a nice agreement between the two approaches has been found confirming the consistency of the method described in [14]. Finally, Fig. 3 shows the electron group velocity extracted from Eq. 3. The approximation of analytical parabolic bands is added in both figures, showing a very limited range of validity, lower than 0.125eV for the $g(E)$ curves, which can be ascribed to the specific shape of the lowest conduction bands. This implies that the full-band numerical structure would be necessary for any specific simulation dealing with higher energies.

3. Discussion

As far as the TCAD framework dealing with the BTE solution, the number of conduction bands N_B usually adopted for Silicon is ≤ 4. In Figs. 4 and 5, $g(E)$ and the product $g(E)u_g(E)$ for Silicon and 4H-SiC are compared, respectively. Dotted vertical lines in Fig. 4 represent the maximum value of the energy at which the approximation with $N_B = 4$ is valid. For silicon, such value is $E = 5.75$eV which is well above the barrier height for

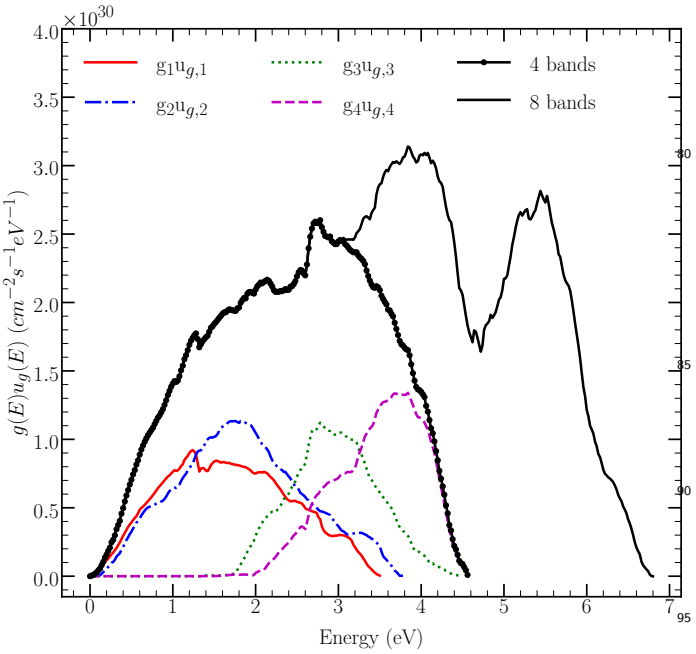

Figure 7: Product $u_g(E)g(E)$ of 4H-SiC calculated according to [14]. Lines corresponding to $g_1u_{g,1}$, $g_2u_{g,2}$, $g_3u_{g,3}$ and $g_4u_{g,4}$ show the contribution of the first 4 bands to $g(E)u_g(E)$, respectively. Black line with circles: $g(E)u_g(E)$ obtained by summing the contribution of the first 4 bands. Black solid line: $g(E)u_g(E)$ calculated accounting for 8 conduction bands.

electrons at the Si/SiO_2 interface ($\Delta E_c \approx 3$eV) meaning that accurate simulations of the most relevant degradation mechanisms can accurately be performed. Differently, the 4H-SiC bands show that the first 4 bands cover an energy range of 3eV only, which is close to the corresponding 4H-SiC/SiO_2 barrier height $\Delta E_c \approx 2.7$eV. The role played by the low-lying conductions bands (g_1, g_2, g_3, g_4) is shown in Fig. 6 together with the sum $\sum_{i=1}^{n} g_i(E)$ for $n = 4$ and $n = 8$. Fig. 7 shows the corresponding values o the product $g(E)u_g(E)$. It is worth noting that a minimum n=4 is required to cover an energy range as large as the band gap of SiC. In particular, a four bands numerical model guarantees an accurate description of $g(E)$ in the range $0 < E < 3$eV which might be valid for electrons experiencing the impact-ionization interactions or the injection into SiO_2. Finally, eight bands can be assumed enough accurate to account for all the hot-carrier degradation mechanisms that can occur in SiC Power MOSFETs at high drain and gate voltages ($0 < E < 7$eV).

4. Conclusion

In this work, the electron group velocity of 4H-SiC has been calculated using DFT simulations. High accuracy has been achieved by calculating the first derivatives of the energy bands through the Wannier90 tool. It has been found that the shape of the two lowest conduction bands makes the validity range of the parabolic band approximation very limited. Differently from Silicon, eight conduction bands are required to guarantee an accurate calculation of the electron density distribution function $f(E)$ up to 7eV. Thus, the knowledge of the group velocity u_g along with g from the full band structure of 4H-SiC is a fundamental ingredient for the modelling of the degradation mechanisms in silicon carbide power MOSFET.

References

[1] She, X., Huang, A.Q., Lucia, O. and Ozpineci, B., 2017. Review of silicon carbide power devices and their applications. IEEE Transactions on Industrial Electronics, 64(10), pp.8193-8205.

[2] Sun, J., Wei, J., Zheng, Z., Wang, Y. and Chen, K.J., 2019, May. Repetitive Short Circuit Energy Dependent V_{TH} Instability of 1.2 kV SiC Power MOSFETs. In 2019 31st International Symposium on Power Semiconductor Devices and ICs (ISPSD) (pp. 263-266). IEEE

[3] Reggiani, S., Barone, G., Poli, S., Gnani, E., Gnudi, A., Baccarani, G., Chuang, M.Y., Tian, W. and Wise, R., 2012. TCAD simulation of hot-carrier and thermal degradation in STI-LDMOS transistors. IEEE Transactions on Electron Devices, 60(2), pp.691-698.

[4] Gnudi, A., Ventura, D., Baccarani, G. and Odeh, F., 1993. Two-dimensional MOSFET simulation by means of a multidimensional spherical harmonics expansion of the Boltzmann transport equation. Solid-state electronics, 36(4), pp.575-581.

[5] Akturk, A., Goldsman, N., Potbhare, S. and Lelis, A., 2009. High field density-functional-theory based Monte Carlo: 4 H-SiC impact ionization and velocity saturation. Journal of Applied Physics, 105(3), p.033703.

[6] Wozny, J., Kovalchuk, A., Lisik, Z., Podgorski, J., Bugalski, P., Kubiak, A. and Ruta, Ł., 2021. Monte Carlo simulations of electron transport in 4H-SiC using the DFT-calculated density of states. Journal of Computational Electronics, 20(2), pp.791-797.

[7] Giannozzi, P., Andreussi, O., Brumme, T., Bunau, O., Nardelli, M.B., Calandra, M., Car, R., Cavazzoni, C., Ceresoli, D., Cococcioni, M. and Colonna, N., 2017. Advanced capabilities for materials modelling with Quantum ESPRESSO. Journal of physics: Condensed matter, 29(46), p.465901.

[8] Perdew, J.P., Burke, K. and Ernzerhof, M., 1996. Generalized gradient approximation made simple. Physical review letters, 77(18), p.3865.

[9] Zhao, G.L. and Bagayoko, D., 2000. Electronic structure and charge transfer in 3C-and 4H-SiC. New Journal of Physics, 2(1), p.16.

[10] Szwacki, N.G., 2017. Structural and electronic properties of silicon carbide polytypes as predicted by exact exchange calculations. Computational Condensed Matter, 13, pp.55-58.

[11] Choudhary, R., Biswas, R., Pan, B. and Paudyal, D., 2019. Defects in SiC for Quantum Computing. MRS Advances, 4(40), pp.2217-2222.

[12] Son, N.T., Chen, W.M., Kordina, O., Konstantinov, A.O., Monemar, B., Janzén, E., Hofman, D.M., Volm, D., Drechsler, M. and Meyer, B.K., 1995. Electron effective masses in 4H SiC. Applied physics letters, 66(9), pp.1074-1076.

[13] Kimoto, T. and Cooper, J.A., 2014. Fundamentals of silicon carbide technology: growth, characterization, devices and applications. John Wiley & Sons.

[14] Gnani, E., Reggiani, S. and Rudan, M., 2002. Density of states and group velocity of electrons in SiO 2 calculated from a full band structure. Physical Review B, 66(19), p.195205.

[15] Mostofi, A.A., Yates, J.R., Pizzi, G., Lee, Y.S., Souza, I., Vanderbilt, D. and Marzari, N., 2014. An updated version of wannier90: A tool for obtaining maximally-localised Wannier functions. Computer Physics Communications, 185(8), pp.2309-2310.